

Preparation and characterization of a stable nano-CoAl₂O₄ ink for glass decoration by ink-jet printing

PENG Xiaojin^{1,2}, ZHANG Qi^{3,4*}, CHENG Jinshu^{1,2}, YUAN Jian^{1,2}, WU Ya^{1,2}, JIE
Junnan^{1,2}

¹State Key Laboratory of Silicate Materials for Architectures, Wuhan University of
Technology, Wuhan, 430070, Hubei, China

²Glass and Technology Research Institute of Shahe, Shahe, 054100, Hebei, China

³State Key Laboratory of Advanced Technology for Materials Synthesis and
Processing, Wuhan University of Technology, Wuhan 430070, Hubei, China

⁴School of Aerospace, Transportation and Manufacturing, Cranfield University,
Cranfield, Bedfordshire, MK430AL, UK

Abstract: A stable inorganic glass ink was prepared by mechanically grinding a mixture of a blue pigment (CoAl₂O₄) and low-melting-point glass powders in a specific organic solvent, which possesses a lower annealing temperature compared with ceramic ink. The CoAl₂O₄ was synthesized by solid-state reaction and the best sintering temperature should be at 1300 °C or above according to the observation of XRD. CoAl₂O₄ shows blue color both in a powder form and coating. The average particle size of pigments and glass powders mixture decreases with the increase of glass powders and milling time. SEM cross-sectional

* Corresponding author. Tel.: 44 (0) 1234 750111; Fax: 44 (0) 1234 751346
E-mail address: Q.Zhang@cranfield.ac.uk

1 images of annealed coating samples illustrate that the pigments are well
2
3 dispersed in the ink layer and the glass adhesive binds well on the surface
4
5 of plate glass materials, enhancing the mechanical strength of the ink
6
7 layer. All the obtained results collectively revealed that the prepared
8
9 nano-CoAl₂O₄ ink can be applied in glass decoration.
10
11
12
13
14
15
16
17
18
19
20
21

22 **Keywords:** Nano-CoAl₂O₄ ink; Preparation; Characterization; Ink-jet
23
24 printing; Glass decoration
25
26
27
28
29
30
31
32
33
34
35
36
37
38
39
40
41
42
43
44
45
46
47
48
49
50
51
52
53
54
55
56
57
58
59
60
61
62
63
64
65

1 Introduction

Ink-jet printing is a non-contact digital printing technology, which can deposit a variety of materials, as droplets, on pre-determined points of a substrate under the control of a computer program. [1~5] One important aspect of ink-jet printing applications is to develop corresponding inks, in which a solute or pigment is dispersed in an organic solvent, with appropriate physical and chemical properties, such as viscosity, surface tension and drop volume of ink and so on. [6~8] Additionally, the use of nano-sized pigments in ink-jet printing system avoids some problems occurring, for example, nozzle clogging and dispersion instability, and thus ensures the quality of printing products. [9~13]

Recently, with an increasing demand of home and public places decorations, colorful patterns on glass tiles with high resolution have attracted the attention of most consumers in the market. The glass decorating materials are often deposited on glasses by means of spin-coating, dip-coating, drop-casting and screen printing previously. However, ink-jet printing as a non-contact deposition method can exhibit obvious advantages over other methods, for instance, a low cost, high definition, efficient use of materials, compatibility with different substrates and its precise when quickly transferring the inks on the surface of substrates. [14] Unfortunately, the reports in the literatures on

1 glass inks are relatively rare in comparison with ceramic inks. Thus
2
3 developing a proper nano-sized inorganic glass ink is essential to ensure
4
5 the operation of ink-jet printing process.
6
7

8
9 Most of the early researching works focused on the preparation of
10
11 ceramic inks and various preparation methods, for example, Guo et al.
12
13 [15] prepared the four colors (CMYK) ceramic inks for ink-jet printing
14
15 by sol-gel method; Domingo et al. [16] prepared a ceramic pigment based
16
17 on Cr and Sb doped TiO_2 by a microemulsion mediated solvothermal
18
19 method; both Merikhi et al. [17] and Dondi et al. [18] prepared
20
21 nano-sized CoAl_2O_4 particles by the polyol method; Kim et al. [19]
22
23 prepared well-dispersed nanoparticles of CoAl_2O_4 for ink-jet printing by a
24
25 hydrothermal process with ultrasonic irradiation; Kuscer et al. [20]
26
27 prepared an aqueous titania suspension for ink-jet printing by mechanical
28
29 grinding method, and so on. Although all these inks are successfully
30
31 applied in printing on ceramics, they fail to perform well on glasses
32
33 because the surface structures of ceramic and glass are totally different,
34
35 the former porous and the latter dense. The different surface structures
36
37 can result in diverse solvent volatilization of ink droplet and discrepant
38
39 coloring effect. What's more, taking the annealing temperature of printed
40
41 substrates into consideration, ceramic substrates allow the annealing at a
42
43 very high temperature which is easy to cause softening and bending
44
45 deformation of glass substrates.
46
47
48
49
50
51
52
53
54
55
56
57
58
59
60
61
62
63
64
65

1 This paper focuses on the preparation of a nano-sized blue glass ink,
2
3 in which cobalt aluminum oxide (CoAl_2O_4) is served as a blue pigment,
4
5 with the aim of annealing ink-jet printed blue materials on glass
6
7 substrates at relatively low temperatures. CoAl_2O_4 is an oxide that
8
9 contains two metallic elements in a spinel structure, where Co^{2+} ions are
10
11 located in tetrahedral positions and Al^{3+} ions are sited in octahedral
12
13 positions. [21~22] Powders of CoAl_2O_4 synthesized by solid-state
14
15 reaction have a unique optical characteristic and excellent resistance to
16
17 light and harsh environment. The addition of low-melting-point glass
18
19 powders to the ink could reduce the annealing temperature, enhance the
20
21 adhesion between pigment and glass substrate, and avoid the softening
22
23 and bending deformation of glass substrate when annealed at high
24
25 temperature.
26
27
28
29
30
31
32
33
34
35
36

37 **2 Materials and Methods**

38 **2.1 Materials**

39
40
41 Aluminum oxide (Al_2O_3), Cobalt (III) oxide (Co_2O_3) and Zinc oxide
42
43 (ZnO) were provided by Sinopharm Chemical Reagent Co., Ltd,
44
45 Shanghai, China. 1, 2-propyleneglycol diacetate, diethylene glycol
46
47 monobutyl ether, polyacrylate, Zinc isoocatanoate isopropanol, ethyl
48
49 alcohol and polysiloxane were purchased from Jianglai Biological Co.,
50
51 Ltd, Shanghai, China. The float glasses were used as substrates for coating.
52
53
54
55
56
57
58
59
60
61
62
63
64
65

1 All other chemicals used in this work were laboratory grade as received
2
3 from Sinopharm Company, China.
4
5

6 **2.2 Preparation of the blue glass inks and coated samples**

7

8
9 The mixtures of 16.6 g Cobalt oxide (Co_2O_3 , 0.1 mol), 20.4 g
10 Aluminum oxide (Al_2O_3 , 0.2 mol) and 1.62 g Zinc oxide (ZnO , 0.02 mol)
11 used for promoting blue coloration were added into 15mL ethyl alcohol
12 and mixed homogeneously into a slurry by milling.
13
14
15
16
17
18

19
20 Subsequently, the slurry was grinded manually for 30 minutes in air
21 until the ethyl alcohol evaporated completely. Following such steps, the
22 obtained mixture was calcined in an alumina crucible at different reaction
23 temperatures (900 °C, 1100 °C, 1200 °C and 1300 °C) for 4 hours in an
24 electrical furnace. The fired product underwent several cycles of grinding
25 and firing in order to achieve a good yield of the required crystalline
26 phase and acceptable homogeneity. The primary pigment (CoAl_2O_4) was
27 obtained when the temperature cooled down to the room temperature.
28
29
30
31
32
33
34
35
36
37
38
39
40
41

42 Additionally, low-melting-point glass, $\text{ZnO-B}_2\text{O}_3\text{-SiO}_2$ system, was
43 used as the glass adhesive to enhance the binding of primary pigments
44 and the surface of plate glass after annealed. Raw materials (ZnO , B_2O_3
45 and SiO_2 , and so on) of low-melting-point glass were mixed by milling
46 and fused in an alumina crucible at 1280 °C for 2 hours to form a high
47 temperature melt. After that, the melt was underwent water quenching
48 and grinded fully. The main chemical compositions of the four different
49
50
51
52
53
54
55
56
57
58
59
60
61
62
63
64
65

1 low-melting-point glasses (Glass Adhesives (GA1~4)) are given in Table
2
3
4 1, with various mass contents of TiO_2 and ZrO_2 . The addition of TiO_2 and
5
6 ZrO_2 can enhance the chemical resistance of ink layer [23, 24], but too
7
8
9 much TiO_2 and ZrO_2 would lead to crystallization of the glass adhesive,
10
11
12 which will interfere the color of pigment [25~27].
13

14 Correspondingly, the primary pigments and low-melting-point glass
15
16 powders were mixed and milled fully using a wet ball-milling method at
17
18 room temperature to form the secondary pigments, which were filtered
19
20 through a 50 μm sieve to remove larger particles and agglomerates. The
21
22 resultant secondary pigments were dispersed in a special organic solvent
23
24 with a vigorously stirring to prepare the homogeneous blue glass ink.
25
26 Table 2 shows the main chemical compositions of the prepared blue glass
27
28
29
30
31
32
33
34
35
36
37
38
39
40
41
42
43
44
45
46
47
48
49
50
51
52
53
54
55
56
57
58
59
60
61
62
63
64
65

66
67
68
69
70
71
72
73
74
75
76
77
78
79
80
81
82
83
84
85
86
87
88
89
90
91
92
93
94
95
96
97
98
99
100
101
102
103
104
105
106
107
108
109
110
111
112
113
114
115
116
117
118
119
120
121
122
123
124
125
126
127
128
129
130
131
132
133
134
135
136
137
138
139
140
141
142
143
144
145
146
147
148
149
150
151
152
153
154
155
156
157
158
159
160
161
162
163
164
165
166
167
168
169
170
171
172
173
174
175
176
177
178
179
180
181
182
183
184
185
186
187
188
189
190
191
192
193
194
195
196
197
198
199
200
201
202
203
204
205
206
207
208
209
210
211
212
213
214
215
216
217
218
219
220
221
222
223
224
225
226
227
228
229
230
231
232
233
234
235
236
237
238
239
240
241
242
243
244
245
246
247
248
249
250
251
252
253
254
255
256
257
258
259
260
261
262
263
264
265
266
267
268
269
270
271
272
273
274
275
276
277
278
279
280
281
282
283
284
285
286
287
288
289
290
291
292
293
294
295
296
297
298
299
300
301
302
303
304
305
306
307
308
309
310
311
312
313
314
315
316
317
318
319
320
321
322
323
324
325
326
327
328
329
330
331
332
333
334
335
336
337
338
339
340
341
342
343
344
345
346
347
348
349
350
351
352
353
354
355
356
357
358
359
360
361
362
363
364
365
366
367
368
369
370
371
372
373
374
375
376
377
378
379
380
381
382
383
384
385
386
387
388
389
390
391
392
393
394
395
396
397
398
399
400
401
402
403
404
405
406
407
408
409
410
411
412
413
414
415
416
417
418
419
420
421
422
423
424
425
426
427
428
429
430
431
432
433
434
435
436
437
438
439
440
441
442
443
444
445
446
447
448
449
450
451
452
453
454
455
456
457
458
459
460
461
462
463
464
465
466
467
468
469
470
471
472
473
474
475
476
477
478
479
480
481
482
483
484
485
486
487
488
489
490
491
492
493
494
495
496
497
498
499
500
501
502
503
504
505
506
507
508
509
510
511
512
513
514
515
516
517
518
519
520
521
522
523
524
525
526
527
528
529
530
531
532
533
534
535
536
537
538
539
540
541
542
543
544
545
546
547
548
549
550
551
552
553
554
555
556
557
558
559
560
561
562
563
564
565
566
567
568
569
570
571
572
573
574
575
576
577
578
579
580
581
582
583
584
585
586
587
588
589
590
591
592
593
594
595
596
597
598
599
600
601
602
603
604
605
606
607
608
609
610
611
612
613
614
615
616
617
618
619
620
621
622
623
624
625
626
627
628
629
630
631
632
633
634
635
636
637
638
639
640
641
642
643
644
645
646
647
648
649
650
651
652
653
654
655
656
657
658
659
660
661
662
663
664
665
666
667
668
669
670
671
672
673
674
675
676
677
678
679
680
681
682
683
684
685
686
687
688
689
690
691
692
693
694
695
696
697
698
699
700
701
702
703
704
705
706
707
708
709
710
711
712
713
714
715
716
717
718
719
720
721
722
723
724
725
726
727
728
729
730
731
732
733
734
735
736
737
738
739
740
741
742
743
744
745
746
747
748
749
750
751
752
753
754
755
756
757
758
759
760
761
762
763
764
765
766
767
768
769
770
771
772
773
774
775
776
777
778
779
780
781
782
783
784
785
786
787
788
789
790
791
792
793
794
795
796
797
798
799
800
801
802
803
804
805
806
807
808
809
810
811
812
813
814
815
816
817
818
819
820
821
822
823
824
825
826
827
828
829
830
831
832
833
834
835
836
837
838
839
840
841
842
843
844
845
846
847
848
849
850
851
852
853
854
855
856
857
858
859
860
861
862
863
864
865
866
867
868
869
870
871
872
873
874
875
876
877
878
879
880
881
882
883
884
885
886
887
888
889
890
891
892
893
894
895
896
897
898
899
900
901
902
903
904
905
906
907
908
909
910
911
912
913
914
915
916
917
918
919
920
921
922
923
924
925
926
927
928
929
930
931
932
933
934
935
936
937
938
939
940
941
942
943
944
945
946
947
948
949
950
951
952
953
954
955
956
957
958
959
960
961
962
963
964
965
966
967
968
969
970
971
972
973
974
975
976
977
978
979
980
981
982
983
984
985
986
987
988
989
990
991
992
993
994
995
996
997
998
999
1000

2.3 Characterization of ink and coating

The CIE- $L^*a^*b^*$ values were measured by spectrophotometer CM-2600d, in which L^* is the lightness axis [black (0), white (100)], a^* is

1 the green (−) to red (+) axis, and b^* is the blue (−) to yellow (+) axis.
2
3 The pH value, surface tension and viscosity of the prepared blue glass ink
4 were measured by Mettler Toledo multi parameter test gauge, Rotary
5 viscosimeter NDJ-5S and Surface tension meter DSAHT17-1,
6
7
8
9
10
11
12
13
14
15
16
17
18
19
20
21
22
23
24
25
26
27
28
29
30
31
32
33
34
35
36
37
38
39
40
41
42
43
44
45
46
47
48
49
50
51
52
53
54
55
56
57
58
59
60
61
62
63
64
65

the green (−) to red (+) axis, and b^* is the blue (−) to yellow (+) axis.
The pH value, surface tension and viscosity of the prepared blue glass ink
were measured by Mettler Toledo multi parameter test gauge, Rotary
viscosimeter NDJ-5S and Surface tension meter DSAHT17-1,
respectively. The crystal structures of primary and secondary pigments
were examined by an X-ray diffraction (XRD, D/MAX-UItimaIV,
Rigaku). The $CuK\alpha$ radiation ($\lambda= 0.15405 \mu\text{m}$) was used at 40 kV and 40
mA. The diffraction patterns were recorded with $2\theta = 10 - 70^\circ$. The
particle size distribution was measured by Mastersizer 2000 (Malvern
Instruments) as well as SEM. The thermal expansion coefficients of the
low-melting-point glasses were measured by thermal expansion analysis.
The cross-sectional morphologies of the coated substrates were observed
by SEM.

3 Results and discussion

3.1 Primary pigment – $CoAl_2O_4$

3.1.1 Effect of solid state reaction temperature on crystallization behavior by XRD analysis

Fig.2 shows the XRD patterns of the calcined pigments at different solid-state reaction temperatures. At 900 °C (Fig.1a), both $CoAl_2O_4$ and Co_3O_4 phases were identified according to their respective JCPD cards (No: 44-0160 and 38-0814) [28]. Increasing the reaction temperature to

1 1100 °C (Fig.1b), CoAl_2O_4 phase became dominant with the existence of
2
3 small amount of Al_2O_3 phase, which was almost invisible when the
4
5
6 reaction temperature was further increased to 1200 and 1300 °C (Fig.
7
8
9 1c&d). The phase analysis manifests that, below 1200 °C, the raw
10
11 materials of Al_2O_3 and Co_2O_3 with a molar ratio of 2:1 failed to form pure
12
13 CoAl_2O_4 but, confirmed by XRD, a solid solution of CoAl_2O_4 and Al_2O_3 .
14
15 Moreover, the intensity of the CoAl_2O_4 diffraction peaks was enhanced
16
17 and the diffraction peaks were sharpened with the increase of reaction
18
19 temperature from 1100 °C to 1300 °C, which were associated with an
20
21 increase in crystallinity.
22
23
24
25
26
27

28 **3.1.2 Chromatic analysis of the primary pigment against different** 29 30 **reaction temperatures** 31 32 33 34 35

36 Table 3 and Fig.3 show the colorimetric $L^*a^*b^*$ values and optical
37
38 pictures of the produced blue primary pigments and a coated sample. L^*
39
40 is the lightness axis [black (0), white (100)], a^* the green (−) to red (+)
41
42 axis, and b^* the blue (−) to yellow (+) axis. In fact, the yield of blue
43
44 color is mainly governed by parameter b^* : the more negative b^* value
45
46 corresponding to the bluer one. According to Fig.3 (a) ~ (d) and Table 1,
47
48 it's easily observed that more intense blue color pigments were achieved
49
50 when the sintering temperature was 1300 °C, which are indicated by the
51
52 extremely high blue component ($b^* = -24.51$) and a relatively low green
53
54
55
56
57
58
59
60
61
62
63
64
65

1 component ($a^* = -1.59$). [9] The color change by varying the reaction
2
3 temperature was well evidenced by the evolution of colorimetric
4
5 parameters. The color of primary pigment achieved at 900 °C (Fig. 3(a))
6
7 was near black while the color of primary pigment at 1100 °C (Fig. 3(b))
8
9 was about navy blue. When the reaction temperature increased from 1200
10
11 °C (Fig. 3(c)) to 1300 °C (Fig. 3(d)), the CoAl_2O_4 pigment presented a
12
13 blue color with more lightness. The color changes of primary pigments at
14
15 different temperatures can attribute to the existence of defects in spinel
16
17 structure. These defects lead to the interchange between Al^{3+} and Co^{2+} in
18
19 tetrahedral and octahedral sites which can change the ligand field around
20
21 the chromophore and hence change the observed color. [29~31] In other
22
23 word, if the preparation of CoAl_2O_4 by solid-state reaction method can be
24
25 executed successfully, the sintering temperature would be about 1300 °C.
26
27 Fig.3 (e) was the coating of primary pigment (d) on a glass substrate,
28
29 which was annealed at 580 °C for 10 minutes. The color of the coating (e)
30
31 is consistent with that of primary pigment (d), indicating that no color
32
33 change of primary pigment occurred during the process of annealing.
34
35

3.2 Secondary pigments - CoAl_2O_4 mixed with glass adhesive

3.2.1 XRD analysis of low-melting-point glasses and secondary pigment

Fig. 4 (A) shows the XRD patterns of low-melting-point glass powders, and Fig.4 (B) shows XRD patterns of the primary pigment (d)

1 (see Table 3) and the secondary pigment (88%). The XRD pattern of
2
3 primary pigment (d) indicates that CoAl_2O_4 is the main crystalline phase,
4
5 with some unknown impurities, possibly being Co_2O_3 or/and Al_2O_3 .
6
7 Low-melting-point glasses 1[#] ~ 4[#] are four different glass adhesives, and
8
9 all the XRD spectra of them (Fig.4 (A)) show that no obvious diffraction
10
11 peaks can be found indicating that they are amorphous and these glass
12
13 adhesives remain amorphous in the secondary pigment (Fig.4 (B)). The
14
15 XRD pattern of the secondary pigment shows the CoAl_2O_4 dominance
16
17 indicating that there is no chemical reaction occurred between glass and
18
19 pigment.
20
21
22
23
24
25
26
27
28

29 **3.2.2 Thermal expansion analysis of low-melting-point glasses**

30
31
32 Fig.5 shows the thermal expansion results of low-melting-point
33
34 glasses 1[#] ~ 4[#]. The thermal expansion coefficients of the four
35
36 low-melting-point glass samples are showed in Table 4, which are all
37
38 close to $9.0 \times 10^{-6}/^\circ\text{C}$ (50~300 °C), the thermal expansion coefficient of the
39
40 plate glass substrate, with an acceptable difference of less than
41
42 $0.3 \times 10^{-6}/^\circ\text{C}$. The consistency of thermal expansion coefficients can avoid
43
44 the crack of glaze film during the process of cooling down after annealed.
45
46
47
48
49
50

51
52 Moreover, the glass transition temperatures (T_g) and the softening
53
54 temperatures (T_s) of the four different glass samples are between 450 °C
55
56 and 500 °C, respectively. If the annealing temperature rises continuously
57
58
59
60
61
62
63
64
65

1 up and over T_s , the glass powders will be melted and turn into molten
2 glass, which fix pigments on the surface of glass substrates. That
3 indicates the practicability of setting the annealing temperature of coated
4 samples at around 580 °C for 10 minutes. [32]
5
6
7
8
9

10
11 T_s and T_g slightly change with the different glass adhesives, which
12 can attribute to the addition of TiO_2 and ZrO_2 in glass raw materials.
13 Although the TiO_2 is an intermediates oxide, it can capture free oxides
14 and transform coordination number from 6 to 4 in order to form
15 tetrahedral structure unit $[TiO_4]$ which can participate in and strength the
16 main Si-O network structures of glass. Meanwhile, the network former
17 ZrO_2 owns high charge cationic Zr^{4+} and clusters negative oxygen ions
18 O^{2-} , which can decrease the quantity of free oxides as well as the ratio of
19 O/Si of $[SiO_4]$ and also enhance the stability of network structures. So the
20 addition of small amount of TiO_2 and ZrO_2 will lead to the decrease of T_s
21 and T_g , without affecting the thermal expansion coefficients substantially.
22
23
24
25
26
27
28
29
30
31
32
33
34
35
36
37
38
39
40
41
42

43 **3.2.3 Particle size analysis of secondary pigment**

44
45 Particle size, distribution of secondary particles, glass adhesive
46 addition and milling time were studied and the results are displayed in
47 Fig.6. Fig.6 (a) and (c) show that adding more glass adhesives or
48 prolonging milling time can reduce the amount of big particles or
49 agglomerates and lead to a narrow, log-normal size distribution. After
50 milling for 16 h, the peak position of distribution graphs decreases
51
52
53
54
55
56
57
58
59
60
61
62
63
64
65

1 gradually to 459 nm from Fig.6 (c), meanwhile, similar results are
2
3 obtained when the glass adhesive content increases to 91%. Additionally,
4
5 the changing trends of mean particle sizes are showed in Fig.6 (b) and (d).
6
7 It's evident that a same decline trend can be observed in both graphs (b)
8
9 and (d), that's to say, the ideal mean particle size (around 500 nm) of
10
11 secondary pigments can be prepared by means of increasing glass
12
13 adhesive additions and milling time, separately or jointly.
14
15
16
17
18
19

20 The surface morphology and particle size distribution of the
21
22 secondary pigments are important factors to the optical dispersion in a
23
24 medium. [9] SEM micrographs of the secondary pigments with 91% of
25
26 glass content and milled for 16h are shown in Fig. 7 (a) and (b),
27
28 respectively. Fig.7 (a) shows that the particles in the secondary pigment
29
30 with a 91% of glass content have an irregular shape with a wide size
31
32 distribution ranging from 100 nm to 1 μm with the mean particle size
33
34 about 0.78 μm . In addition, Fig.7 (b) illustrates the particle size
35
36 distribution of secondary pigment after being milled for 16 h, and the
37
38 same irregular shape can be observed, but the mean particle size is about
39
40 0.50 μm . Therefore, it can be concluded that the way of increasing the
41
42 milling time is efficient.
43
44
45
46
47
48
49
50
51

52 **3.3 Glass ink**

53 **3.1 Viscosity of the prepared glass ink**

54
55
56
57
58
59
60
61
62
63
64
65

1 Viscosity mainly affects the rheological characteristics of the glass ink
2
3 when it circulates through the capillary nozzles of printer. A high
4
5 viscosity could lead to an insufficient jet of ink, whereas a significantly
6
7 small viscosity could degrade inner resistance of the ink, which makes the
8
9 ink drop crescent shaped, resulting in damped oscillation. [2, 33] The
10
11 viscosity of prepared blue glass ink was measured to be 28.45 mPa·s at
12
13 room temperature, which allowed the glass ink to be printed well when
14
15 flowing through the nozzles of the printer head and forming drops with
16
17 proper physics and fluid mechanics performance during the printing
18
19 process. [34, 35]
20
21
22
23
24
25
26

27 **3.2 Surface tension of the prepared glass ink**

28
29
30
31
32
33 Surface tension is another physical parameter measured for the
34
35 printing performance of the prepared inks, which mainly affects the
36
37 decomposition into fine drops of glass ink efflux through the capillary
38
39 tube of the printer nozzle during printing process. The diethylene glycol
40
41 monobutyl ether, as a major phase in the glass ink formulation, plays a
42
43 decisive role in controlling the surface tension. According to recent
44
45 literatures, the suitable range for surface tension is in between 20 to 70
46
47 mN·m⁻¹. [3, 11] The surface tension of the prepared blue glass ink was
48
49 measured to be 29.18 mN·m⁻¹ at pH = 7.5, placing it within a range of the
50
51 preferred value for ink-jet printing.
52
53
54
55
56
57
58
59
60
61
62
63
64
65

3.3 Main required properties for drop-on-demand printing ink

Particle size, viscosity, surface tension and pH are the four basic properties to evaluate whether the ink is suitable for drop-on-demand ink-jet printing. Limiting the particle size less than $1\mu\text{m}$ would effectively avoid blockages in nozzles of the printer. Viscosity mainly affects the flowing property of ink both in cartridge and pipe, while surface tension mainly controls the drop-forming process from the nozzle. The alkaline ink can prevent the printing nozzles being corroded. Table 5 shows the comparison of main required physical and chemical properties of drop-on-demand ink and blue glass ink. The results show that these physical and chemical values of our blue glass ink are within the normal ranges of the drop-on-demand printing ink, [11] indicating that our blue glass ink is applicable in ink-jet printing.

3.4 SEM analysis of cross section of the coating sample

SEM cross section images of the coating samples are shown in Fig.8, which clearly demonstrate the close connection between the ink layer and the substrate without any cracks or air pores. Fig.8 (a) shows the cross-sectional uniformity in the thickness of the ink layer on the plate glass slides, and at the same time, shows that the nano- CoAl_2O_4 pigments are well dispersed in the glaze layer. The interface between the glass and the glaze is displayed in Fig.8 (a) and (b). Two SEM images show a good

1 bonding between ink materials and the glass substrate, thanks to the
2
3 assistance of low melting point glass phase.
4
5

6 7 **4 Conclusions** 8 9

10 We have demonstrated in this paper that a stable nano-CoAl₂O₄ ink
11 that meets the ink-jet printing requirements is successfully synthesized by
12 mechanically grinding pigments and glass phase powders.
13
14
15
16
17

18 (a) The optimal reaction temperature for synthesizing CoAl₂O₄
19 pigment by solid-state reaction was 1300 °C and the L*a*b* values of
20 CoAl₂O₄ pigment were 35.75, -0.75, -24.51, respectively, indicating a
21 blue color.
22
23
24
25
26
27
28

29 (b) Glass adhesive of ZnO-B₂O₃-SiO₂ system was used to enhance
30 the binding of pigments on the surface of the substrates. T_g and T_s of
31 glass adhesive are at about 450 °C and 500 °C, respectively. The thermal
32 expansion analysis is about 9.0*10⁻⁶/ °C (50~300 °C), similar to that of
33 glass substrate, ensuring the crack-free coating
34
35
36
37
38
39
40
41
42

43 (c) Small particles that are in favor of ink-jet printing can be
44 obtained by milling pigment and glass adhesives together for 16 h.
45
46
47

48 (d) Surface tension of the prepared blue glass ink was measured to
49 be 29.18 mN·m⁻¹ at pH=7.5, while viscosity of this glass ink was
50 8.21mPa·s, which fall in the range of the preferred values for ink-jet
51 printing glass inks.
52
53
54
55
56
57
58
59
60
61
62
63
64
65

1 (e) Coated samples show that pigments are well dispersed in the ink
2
3 layer and the prepared glass ink binds well on the surface of plate glass
4
5 materials, enhancing the mechanical strength of the ink layer.
6
7
8
9

10 11 12 13 14 15 16 **Acknowledgements** 17

18
19
20 The authors acknowledge the financial support given by Glass and
21
22 Technology Research Institute of Shahe.
23
24
25
26
27
28
29
30
31
32
33
34
35
36
37
38
39
40
41
42
43
44
45
46
47
48
49
50
51
52
53
54
55
56
57
58
59
60
61
62
63
64
65

References

- [1] Hosseini ZM, Soleimani-Gorgani A (2012) Ink-jet printing of micro-emulsion TiO₂ nano-particles ink on the surface of glass. *J Eur Ceram Soc* 32: 4271-4277
- [2] Soleimani-Gorgani A, Ghahari M, Peymannia M (2015) In situ production of nano-CoAl₂O₄ on a ceramic surface by ink-jet printing. *J Eur Ceram Soc* 35: 779-786
- [3] Zhao X, Evans JRG, Edirisinghe MJ, Song JH (2003) Formulation of a ceramic ink for a wide-array drop-on-demand ink-jet printer. *Ceram Int* 29: 887-892
- [4] Grau J, Cima M, Sachs E (1996) Fabrication alumina molds for slip casting and 3-D printing. *Ceram Ind* 146(7): 22-27
- [5] Teng WD and Edirisinghe MJ (1998) Development of ceramic inks for direct continuous jet printing of ceramics. *Ceram Trans* 81(4): 1033-1036
- [6] Kosmala A, Wright R, Zhang Q, Kirby P (2011) Synthesis of silver nano particles and fabrication of aqueous Ag inks for inkjet printing. *Mater Chem Phys* 129: 1075-1080
- [7] Menning M, Kalleder A, Jonschker G, Schmidt H (1997) Sol-gel coatings for the substitution of fluoride or lead containing white decorations on glass. *J Non-Cryst Solids* 218: 395-398
- [8] Kettle J, Lamminmäki T, Gane P (2010) A review of modified surfaces for high speed inkjet coating. *Surf Coat Technol* 204: 2013-2109
- [9] Chouiki M, Schoeftner R (2011) Inkjet printing of inorganic sol-gel ink and control of the geometrical and characteristics. *J Sol-Gel Sci Technol* 58: 91-95

- 1 [10] Cavalcante PMT, Dondi M, Guaini G, Raimondo M, Baldi G (2009) Colour
2 performance of ceramic nano-pigments *Dyes & Pigment* 80: 226-232
3
4
5
6 [11] Gardini D, Dondi M, Costa AL, Matteucci F, Blosi M, Galassi C (2008)
7 Nano-sized ceramics inks for drop-on-demand ink-jet printing in quadrichromy. *J*
8
9 *Nanosci Nanotechnol* 8 (4) : 1979-1988
10
11
12
13
14 [12] Fasaki I, Siamos K, Arin M, Lommens P, Van Driessche I, Hopkins SC,
15 Glowacki BA, Arabatzis I (2012) Ultrasound assisted preparation of stable
16 water-based nanocrystalline TiO₂ suspensions for photocatalytic applications of
17 inkjet-printed films. *Appl Catal A* 411-412: 60-69
18
19
20
21
22
23
24
25 [13] Akdemir S, Ozel E, Suvaci E (2011) Solubility of blue CoAl₂O₄ ceramic pigments
26 in water and diethylene glycol media. *Ceram Int* 37: 863-870
27
28
29
30
31 [14] Ma SH, Matrick H, Shor AC, Spinelli HJ, Sheard ME, Hochberg J (1993)
32 Aqueous pigmented ink for ink jet printer. US Patent 5221334
33
34
35
36 [15] Guo YJ, Zhou ZJ, Yang ZF (2002) Physicochemical properties of coloured
37 ceramic ink used for continuous ink-jet printing by sol-gel method. *China Ceramic*
38 38: 17-19
39
40
41
42
43
44 [16] Jovaní M, Domingo M, Machado TR, Longo E, Mir HB, Cordocillo E (2015)
45 Pigments based on Cr and Sb doped TiO₂ prepared by microemulsion-mediated
46 solvothermal synthesis for inkjet printing on ceramic. *Dyes & Pigment*. 116:
47 106-113
48
49
50
51
52
53
54
55 [17] Merikhi J, Jungk HO, Feldmann C (2000) Sub-micrometer CoAl₂O₄ pigment
56 particles-synthesis and preparation of coatings. *J Mater Chem* 10: 1311-1314
57
58
59
60
61
62
63
64
65

- 1 [18] Dondi M, Blosi M, Gardini D, Zanelli C (2012) Ceramic pigments for digital
2 decoration inks: an overview. *Ceramic Forum International* 8: 59-64
3
4
5
6 [19] Kim JH, Son BR, Yoon DH, Hwang KT, Noh HG, Cho WS, Kim US (2012)
7
8
9 Characterization of blue CoAl_2O_4 nano-pigment synthesized by ultrasonic
10 hydrothermal method. *Ceram Int* 38: 5707-5712
11
12
13
14 [20] Kuscer D, Ozkol G, Trefalt G, Kosec M (2012) Formulation of an aqueous
15
16
17 titania suspension and its patterning with ink-jet printing technology. *J Am Ceram*
18
19
20 *Soc* 95: 487-493
21
22
23 [21] Burdett JK, Price GD, Price SL (1982) Role of the crystal-field theory in
24
25
26 determining the structures of spinels. *J Am Chem Soc* 104: 92-94
27
28
29 [22] Wang C, Liu S, Liu L, Bai X (2006) Synthesis of cobalt-aluminate spinels via
30
31
32 glycine chelated precursors. *Mater Chem Phys* 96: 361-410
33
34 [23] Manfredo LJ, McNally RN (1984) The corrosion resistance of high ZrO_2
35
36
37 fusion-cast Al_2O_3 - ZrO_2 - SiO_2 glass refractories in soda lime glass. *J Mater Sci* 19:
38
39
40 1272-1276
41
42 [24] Matsuda A, Matsuno Y, Katayama S (1989) Weathering resistance of glass plates
43
44
45 coated with sol-gel derived 9TiO_2 - 91SiO_2 films. *J Mater Sci* 8: 902-904
46
47
48 [25] Cheng JS, Kang JF, Lou XC, Zhang XM, Liu K (2015) Effect of TiO_2 on
49
50
51 crystallization of the glass ceramics prepared from granite tailings. *Journal of*
52
53
54 *Wuhan University of Technology-Mater Sci Ed* 30: 22-26
55
56 [26] Cheng HZ, Lin HJ, Wang MC, Lu P (2015) Influences of TiO_2 addition on the
57
58
59 crystallization behavior, microstructure and magnetic properties of
60
61
62
63
64
65

1 Li₂O-MnO₂-Fe₂O₃-CaO-P₂O₅-SiO₂ glasses. Metal Mater Trans A 46: 2040-2050
2

3 [27] Strukelj E, Comte M, Roskosz M, Richet P (2015) Effect of zirconium on the
4 structure and congruent crystallization of a super cooled calcium aluminosilicate
5 melt. J Am Chem Soc 98: 1942-1950
6
7
8
9

10 [28] Greenstein LM (1988) Properties and Economics, in Pigment Handbook, ed. by
11 P.A. Lewis. Volume 1, 2nd pp829-858
12
13
14
15
16

17 [29] Granados NB, Yi E, Laine R, Baena ORJ (2015) CoAl₂O₄ blue nanopigments
18 prepared by liquid-feed flame spray pyrolysis method. Matéria, pp580-587
19
20
21

22 [30] Ahmed IS, Dessouki HA, Ali AA (2008) Synthesis and characterization of new
23 nano-particles as blue ceramic pigment, Spectrochimica Acta Part A 71: 616-620
24
25
26
27

28 [31] Cunha JD, Melo DMA, Martinelli AE, Melo MAF, Maia I, Cunha SD (2005)
29 Ceramic pigment obtained by polymeric precursors. Dyes & Pigments. 65: 11-14
30
31
32

33 [32] Tool AQ (1946) Relation Between Inelastic Deformability and Thermal
34 Expansion of Glass. J Am Chem Soc 29: 240-253
35
36
37
38

39 [33] Peymannia M, Soleimani-Gorgani A, Ghahari M, Najafi F (2014) Production of a
40 stable and homogeneous colloid dispersion of nano-CoAl₂O₄ pigment for
41 ceramic ink-jet ink. J Eur Ceram Soc 34: 3119-3126
42
43
44
45
46

47 [34] Derby B (2010) Inkjet printing of functional and structural materials-fluid
48 property requirements, feature stability and resolution. Annu Rev Mater Sci 40:
49 395-414
50
51
52
53
54

55 [35] Martin GD, Hoath SD, Hutchings IM (2008) Inkjet printing-the physics of
56 manipulating liquid jets and drops. J Phys Conf Ser 105: 012001
57
58
59
60
61
62
63
64
65

Figure captions

Fig.1 The flowchart of the whole preparing processes of blue glass ink and glass surface coating

Fig.2 XRD patterns of the CoAl_2O_4 powders at different reaction temperatures: (a) 900 °C; (b)1100 °C; (c)1200 °C; (d)1300 °C

Fig.3 Pictures of the prepared primary pigments (a) ~ (d) and coated sample (e)

Fig.4 XRD patterns of (A) low-melting-point glass (1) ~ (4);

(B) Primary pigment (d) and secondary pigment (88%)

Fig.5 Thermal expansion curves of low-melting-point glasses 1# ~ 4#;

Fig.6 Size distribution curves of secondary pigments under different conditions:

(a) Effect of different glass adhesives additions on distribution of secondary pigments;

(b) Changing trend of mean particle size with different glass adhesive additions;

(c) Effect of different milling times on distribution of secondary pigments;

(d) Changing trend of mean particle size with different milling times;

Fig.7 SEM micrographs of the milled pigments with different treatments: (a) 91% glass contents; (b) 16h of milling

Fig.8 SEM images of printing sample: magnification X2000(a) and X5000(b)

Figures:

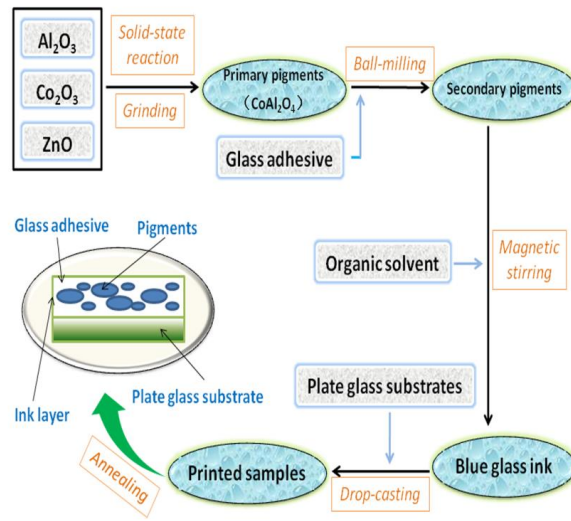


Fig. 1

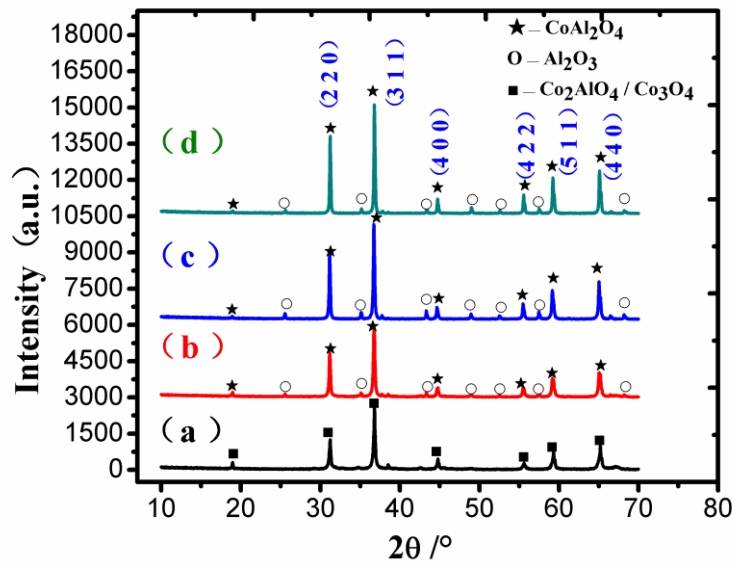


Fig. 2

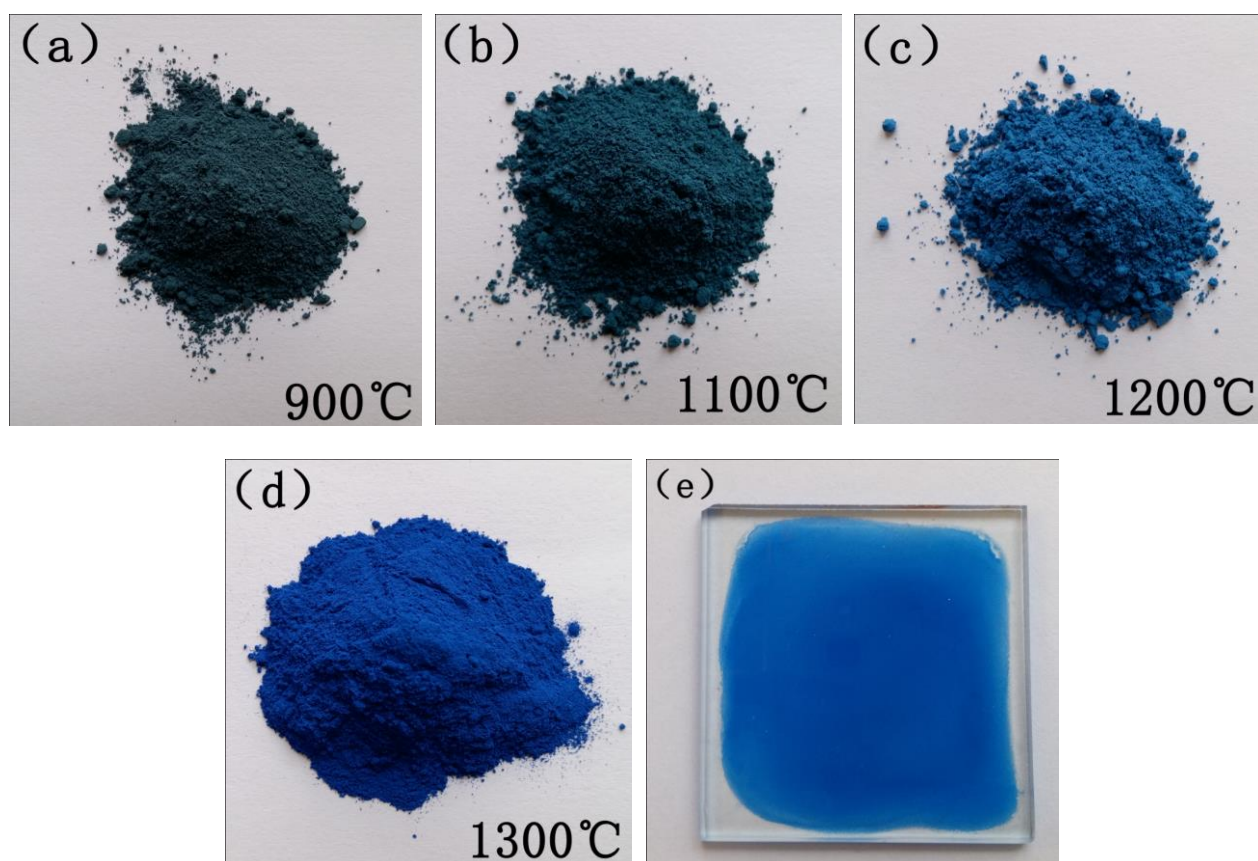


Fig. 3 (a), (b), (c), (d) and (e)

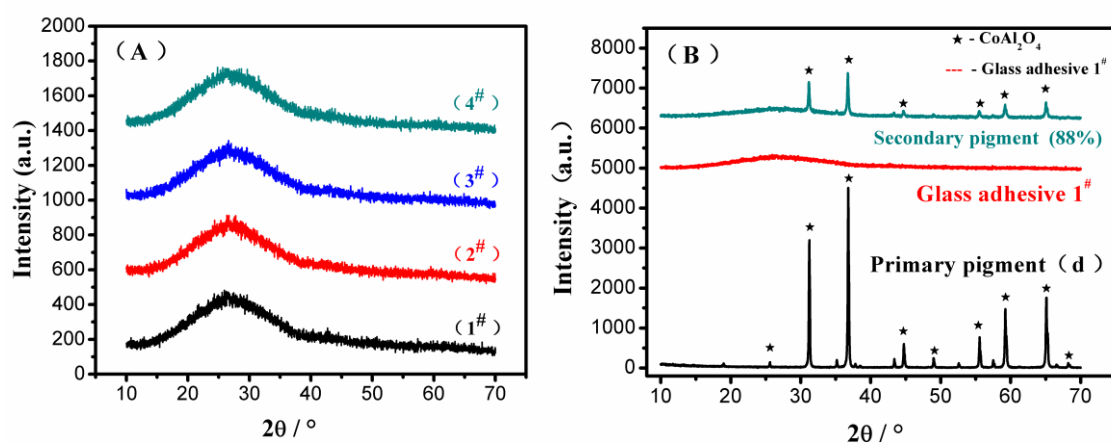


Fig. 4 (A) and (B)

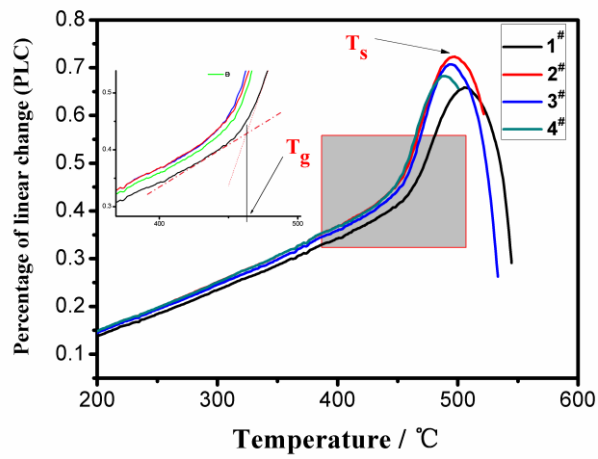


Fig. 5

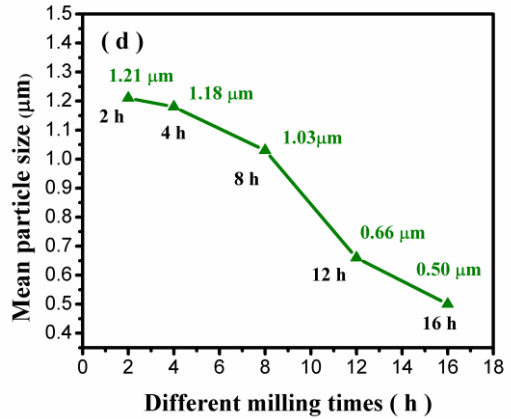
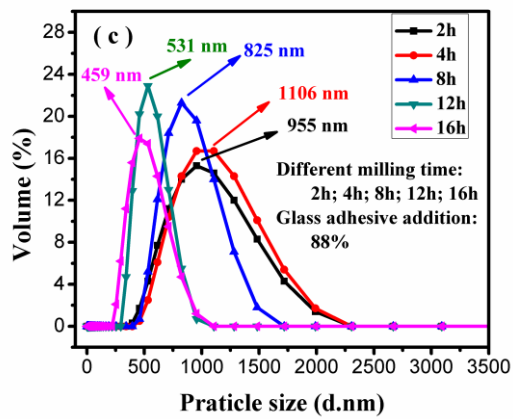
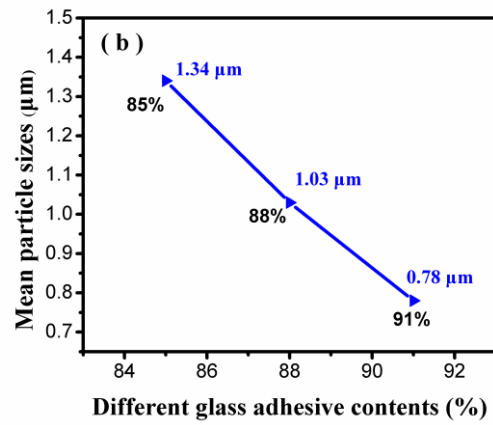
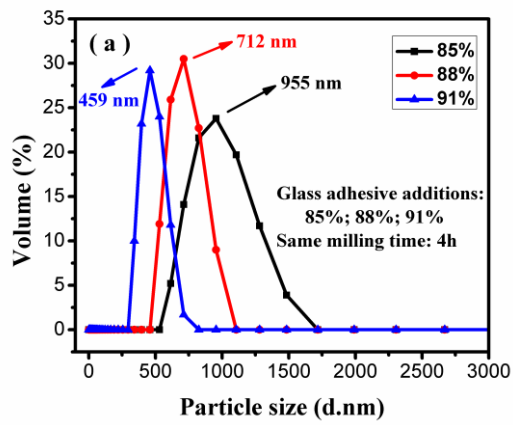


Fig. 6 (a), (b), (c) and (d)

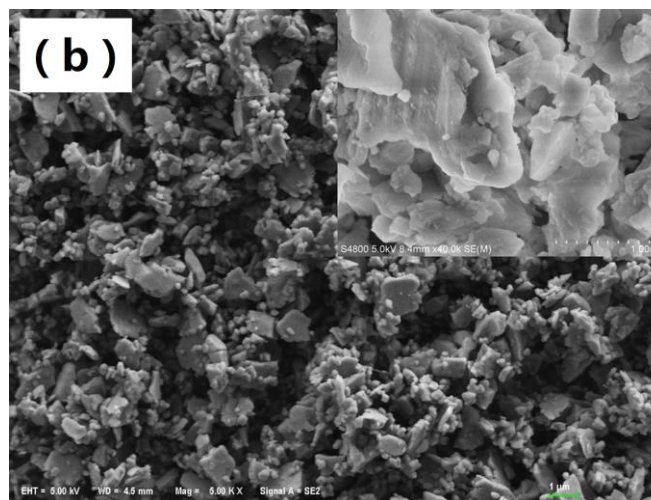
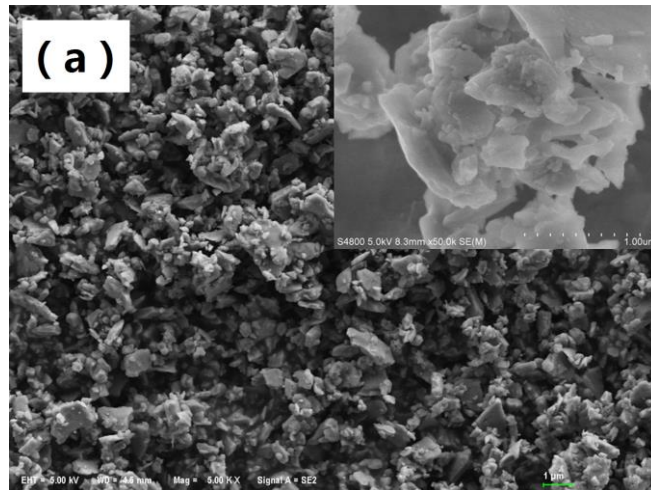


Fig. 7 (a) and (b)

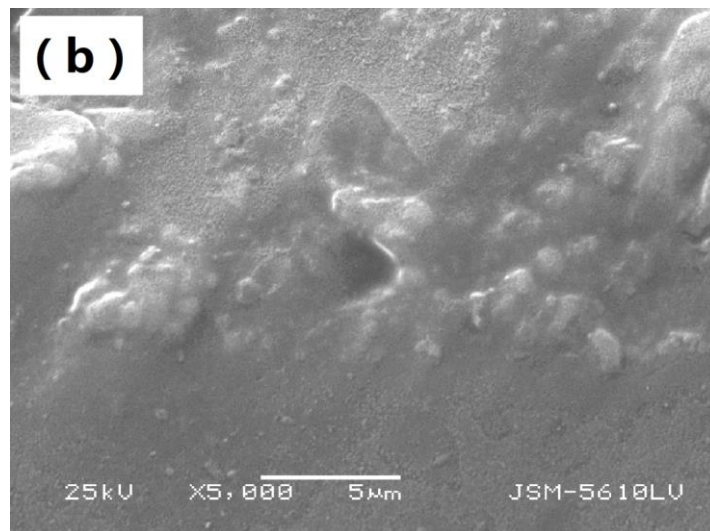
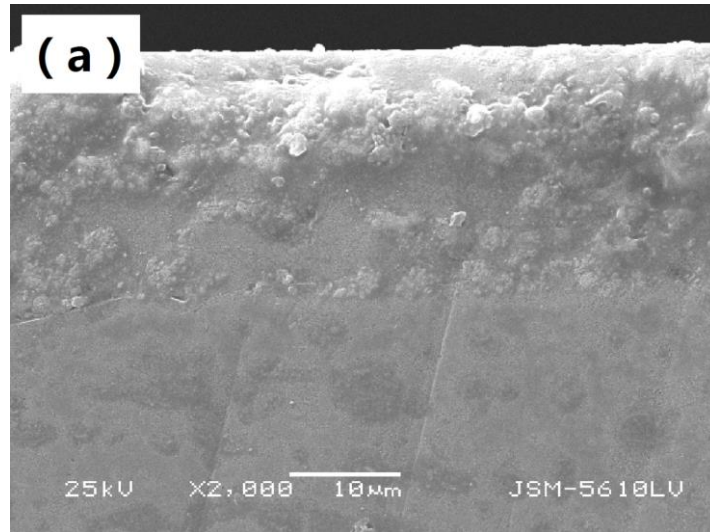


Fig. 8 (a) and (b)

Table captions:

Table 1 Chemical compositions of low-melting-point glass /wt%

Table 2 Chemical compositions of the prepared blue glass ink/wt%

Table3 L*a*b* values of primary pigments (a), (b), (c) and (d)

Table 4 Thermal expansion coefficients of the four different glass adhesives

Table5 Comparison of main required properties of inks

Tables:

Table 1

	SiO ₂	B ₂ O ₃	ZnO	Al ₂ O ₃	Li ₂ O	Na ₂ O	K ₂ O	CaO	BaO	TiO ₂	ZrO ₂
GA-1	41.24	17.53	17.53	3.08	6.19	6.70	3.61	2.57	1.55	2	1
GA-2	41.24	17.53	17.53	3.08	6.19	6.70	3.61	2.57	1.55		1
GA-3	41.24	17.53	17.53	3.08	6.19	6.70	3.61	2.57	1.55	2	
GA-4	41.24	17.53	17.53	3.08	6.19	6.70	3.61	2.57	1.55		

Table 2

	Primary pigment	4.29%	
	Glass adhesive	31.43%	
Solvent	1,2-Propylene glycol diacetate	C ₇ H ₁₂ O ₄	17.36%
	Diethylene glycol monobutyl ether	C ₈ H ₁₈ O ₃	41.76%
	Polyacrylate	C ₃ H ₄ O ₂ (C ₃ H ₆ O) _n	3.54%
	Zinc isoocatanoate	C ₁₆ H ₃₀ O ₄ Zn	1.61%
	Polysiloxane	[R _n SiO _{4-n/2}] _m	0.01%

Table3

Primary pigment	L*	a*	b*
(a)	26.24	-0.42	-7.84
(b)	28.72	-0.48	-16.11
(c)	33.26	-0.75	-20.34
(d)	35.75	-1.59	-24.51

Table 4

	Thermal expansion coefficient
1#	8.704*10 ⁻⁶
2#	9.246*10 ⁻⁶
3#	9.086*10 ⁻⁶
4#	9.229*10 ⁻⁶

Table5

	Drop-on-demand printing ink	Blue glass ink
Maximum particle size	< 1μm	500 nm
Viscosity (mPa·s)	1 ~ 30	8.21
Surface tension (mN·m ⁻¹)	20 ~ 70	29.18
pH	7 ~ 12	7.5

Preparation and Characterization of a Stable Nano-Sized $Zn_xCo_{1-x}Al_2O_4$ Ink for Glass Decoration by Ink-jet Printing

Peng, Xiaojin

2017-06

Attribution-NonCommercial 4.0 International

Xiaojin Peng, Qi Zhang, Jinshu Cheng, Jian Yuan Ya Wu and Junnan Jie. Preparation and Characterization of a Stable Nano-Sized $Zn_xCo_{1-x}Al_2O_4$ Ink for Glass Decoration by Ink-jet Printing. *Fizika i Khimiya Stekla / Glass Physics and Chemistry*, May 2017, Vol.43, Iss.3, pp246-256
<http://dx.doi.org/10.1134/S1087659617030105>

Downloaded from CERES Research Repository, Cranfield University